HHS Public Access

Author manuscript

J Cell Physiol. Author manuscript; available in PMC 2018 March 13.

Published in final edited form as:

J Cell Physiol. 2016 April ; 231(4): 896–907. doi:10.1002/jcp.25181.

Kidney Injury Molecule-1 Enhances Endocytosis of Albumin in Renal Proximal Tubular Cells

Xueying Zhao[*], **Chen Jiang**, **Rebecca Olufade**, **Dong Liu**, and **Nerimiah Emmett**

Department of Physiology, Morehouse School of Medicine, Atlanta, Georgia

Abstract

Receptor-mediated endocytosis plays an important role in albumin reabsorption by renal proximal tubule epithelial cells. Kidney injury molecule-1 (KIM-1) is a scavenger receptor that is upregulated on the apical membrane of proximal tubules in proteinuric kidney disease. In this study, we examined the cellular localization and functional role of KIM-1 in cultured renal tubule epithelial cells (TECs). Confocal immunofluorescence microscopy reveals intracellular and cell surface localization of KIM-1 in primary renal TECs. Albumin stimulation resulted in a redistribution of KIM-1 and tight junction protein zonula occludens-1 in primary TEC monolayer. An increase in albumin internalization was observed in both primary TECs expressing endogenous KIM-1 and rat kidney cell line (NRK-52E) overexpressing exogenous KIM-1. KIM-1-induced albumin accumulation was abolished by its specific antibody. Moreover, endocytosed KIM-1 and its cargo proteins were delivered from endosomes to lysosomes for degradation in a clathrin-dependent pathway. Supportive evidence includes (1) detection of KIM-1 in Rab5-positive early endosomes, Rab7-positive late endosomes/multivesicular bodies, and LAMP1-positive lysosomes, (2) colocalization of KIM-1 and clathrin in the intracellular vesicles, and (3) blockade of KIM-1-mediated albumin internalization by chlorpromazine, an inhibitor of clathrin-dependent endocytosis. KIM-1 expression was upregulated by albumin but downregulated by transforming growth factor-β1. Taken together, our data indicate that KIM-1 increases albumin endocytosis in renal tubule epithelial cells, at least partially via a clathrin-dependent mechanism.

During progression of proteinuria and kidney injury, the accumulation of certain proteins in the lysosomes of the proximal tubules are thought, via mediators, to induce inflammation and fibrogenesis in the interstitium (Remuzzi and Bertani, 1998). Filtered albumin is mainly reabsorbed from the proximal tubular lumen by receptor-mediated endocytosis. There are three major endocytic pathways involved in receptor-mediated endocytosis with respect to vesicle formation: (1) endocytosis via clathrin-coated pits, (2) caveolae-mediated endocytosis, and (3) clathrin- and caveolae-independent endocytosis by a largely unknown mechanism (Mukherjee et al., 1997; Schmid, 1997; Conner and Schmid, 2003; Gekle, 2005). In renal proximal tubule epithelial cells (TECs), clathrin-mediated endocytosis is the predominant pathway for uptake of filtered proteins (Gekle et al., 1997; Gekle, 1998; Christensen and Birn, 2002).

[*]Correspondence to: Xueying Zhao, Department of Physiology, Morehouse School of Medicine, Atlanta, GA. xzhao@msm.edu.

Megalin and cubilin are the major scavenger receptors for physiologic reabsorption of filtered albumin by proximal tubular cells (Christensen and Willnow, 1999; Birn et al., 2000a; Birn et al., 2000b; Zhai et al., 2000; Verroust and Kozyraki, 2001; Amsellem et al., 2010). The megalin-cubilin complex accepts a variety of ligands including albumin, vitamin binding proteins, hormone binding proteins, hormones, and light chains (Christensen et al., 1999; Christensen and Willnow, 1999). Cubilin and/or megalin-deficient mice exhibited markedly decreased uptake of albumin by proximal tubule cells and resultant albuminuria (Amsellem et al., 2010). Additionally, analysis in megalin knockout mosaic mice revealed that megalin-positive tubular cells preferentially accumulated albumin and expressed injury markers following glomerular podocyte injury (Motoyoshi et al., 2008). However, a recent report indicate that increased albumin accumulation in the lysosomes of proximal tubules after onset of proteinuria is associated with unchanged levels of megalin and cubilin in a mouse model of focal segmental glomerulosclerosis (Nielsen et al., 2013), suggesting that megalin/cubilin complex may not be responsible for abnormally high protein trafficking in proteinuric kidney disease.

Recently, CD36, a class B scavenger receptor, has been shown to be upregulated and act as a novel mediator influencing binding and uptake of albumin in the proximal tubule in proteinuric renal disease (Baines et al., 2012). Similar to CD36, as an epithelial scavenger receptor, kidney injury molecule-1 (KIM-1) or T-cell Ig and mucin domain (TIM-1, also known as HAVCR1) is robustly induced in activated proximal tubular epithelium in proteinuric, toxic and ischemic kidney diseases (Kuehn et al., 2002; van Timmeren et al., 2006; Kramer et al., 2007, 2009; Bonventre, 2009; Chaturvedi et al., 2009). Our previous studies performed in a rat model of type 2 diabetes indicated that KIM-1 protein was gradually increased and mainly present on the apical membrane of proximal tubular epithelium during the progression of proteinuria (Li et al., 2010; Zhao et al., 2011), whereas its level was negligible in the kidney of normal rats. KIM-1 expression on the apical membrane of tubular epithelium following injury to the kidneys has been shown to confer endocytic and phagocytic phenotypes on epithelial cells with resultant internalization of lipoproteins and apoptotic cells (Ichimura et al., 2008). Therefore, we hypothesized that KIM-1 might serve as an endocytic scavenger of filtered protein, notably albumin, in proteinuric kidney disease. The present study was designed to investigate the role of KIM-1 in albumin uptake by proximal tubular cells and to characterize the intracellular compartments through which endocytosed KIM-1 and cargo proteins are processed.

Materials and Methods

Animals

Male C57BL/6 mice were purchased from Charles River Laboratories (Wilmington, Mass.). The animals were housed in a temperature-controlled room with a 12:12-h light–dark cycle and free access to normal mouse chow and water. All animal protocols were approved by the Institutional Animal Care and Use Committee and were in accordance with the requirements stated in the National Institutes of Health Guide for the Care and Use Laboratory Animals.

Reagents

Antibodies specifically against human KIM-1 (hKIM-1: AF1750, less than 0.1% cross-reactivity with recombinant mouse or rat KIM-1), rat KIM-1 (rKIM-1: AF3689, less than 1%cross-reactivity with recombinant hKIM-1), and mouse KIM-1 (mKIM-1: AF1817, less than 5% cross-reactivity with recombinant hKIM-1) were purchased from the R&D Systems (Minneapolis, MN). Antibodies against clathrin heavy chain and caveolin-1 were from Abcam Inc. (Boston, MA). Anti-β-actin antibody, chlorpromazine, and bovine serum albumin (BSA) were from Sigma–Aldrich (St. Louis, MO). In addition to antibodies against tight junction protein zonula occludens (ZO)-1, other reagents including CellLight Early Endosome Rab5a-GFP, Late Endosome Rab7a-red fluorescent protein (RFP), and lysosomal associated protein 1 (LAMP1)-GFP BacMam 2.0, BSA conjugated with fluorescein isothiocyanate (FITC-BSA, green) or Alexa Fluor 594 (AF594-BSA, red), Dextran (10kDa) conjugated with Alexa Fluor 594 (AF594-dextran, red), Lysotracker, and all tissue culture reagents were from Life Technologies (Carlsbad, CA).

Cell culture and transfection

Normal renal proximal tubular cell lines from rat (NRK-52E) and human (HK-2) were purchased from the American Type Culture Collection (Monassas, VA), and the cells were maintained in DMEM/F12 supplemented with 10% FBS, 2 mM L-glutamine, 100 U/ml penicillin, and 100 μg/ml streptomycin. Cells were subcultured (passage number < 30) twice a week on reaching confluency.

Human KIM-1 coding sequence was obtained from ORF Gateway Entry and subcloned into pcDNA-DEST or enhanced GFP-tagged pLenti7.3-DEST vector (Life Technologies) for expression in mammalian cells. NRK-52E cells were transiently transfected with hKIM-1 constructs at ~ 50% confluence using Lipofectamine 2000 reagent (Life Technologies) according to the manufacturer's instruction. Plasmid DNA/Lipofectamine mixtures were added to the cells in 35-mm glass-bottom culture dishes. Similar to published studies (Zeng et al., 2012; Sandbichler et al., 2013), the transfection efficacy of NRK-52E cells with lipofectamine 2000 was 23%.

Primary culture of proximal tubule epithelial cells

Primary renal TECs were prepared from C57BL/6 mouse kidneys as described previously (Baines et al., 2012). Briefly, tubular fragments were collected and suspended in DMEM/F12 medium, supplemented with 5% FBS, penicillin, and streptomycin. To test the effects of albumin or TGF-β1 on KIM-1 expression, 80% confluent cells (day 6) were washed with serum-free DMEM and incubated in culture medium with BSA (10 mg/ml) or TGF-β1 (1 or2 ng/ml). The preparation of BSA has been shown to be essentially fatty acid free and low endotoxin by the manufacturing company and its concentration is similar to that used in previous studies (Wang et al., 1997; Zoja et al., 1998; Erkan et al., 2001).

Protein extraction and Western blot analysis

Whole-cell extracts were prepared by scraping cells in ice-cold RIPA buffer (50 mM Tris-HCl pH 7.4, 150 mM NaCl, 1% NP-40, 0.5% sodium deoxycholate, 0.1% SDS, 1 mM phenylmethylsulfonylfluoride PMSF, and 1 mM Na_3VO_4 supplemented with proteinase

inhibitor cocktail from Sigma–Aldrich). The lysate was centrifuged at 12,000 × g for 10 min at 4°C and protein concentration was determined by the Bradford method (Bio-Rad Laboratories, Hercules, CA). Proteins were separated by electrophoresis on a 10% stacking Tris-glycine gel and transferred to a nitrocellulose membrane. The primary antibodies were goat anti-hKIM-1 (1:1000), anti-mKIM-1 IgG (1:1000), rabbit anti-phospho Smad3 (1:500), anti-E-cadherin (1:1000, Cell Signaling, Danvers, MA), and mouse anti-β-actin antibody (Sigma–Aldrich). The blots were then washed in PBS-0.3% Tween-20 and incubated with the second antibody (donkey anti-goat, anti-rabbit, or anti-mouse IgG) conjugated to horseradish peroxidase for 90 min at room temperature and washed. Detection was accomplished by enhanced chemiluminescence Western blotting (ECL, Amersham), and blots were exposed to X-ray film (Hyperfilm-ECL, Amersham). Western blots were quantified by densitometry (Scion Image for Windows, Scion Corporation, Fredrick, MD).

Immunofluorescence staining

To evaluate KIM-1 expression and localization, primary TECs or HK-2 cells were grown to confluence on coverslips. The cells were washed with ice-cold PBS (pH 7.4), fixed in 4% paraformaldehyde, and permeabilized with 0.2% Trixton x-100. For double staining, the cells were incubated with primary antibodies of goat anti-mKIM-1 (1:100) and rabbit anti-ZO-1 (1:50), rabbit anti-clathrin (1:100), or rabbit anti-caveolin-1 (1:100) overnight at 4°C. After washing with PBS, the cells were then incubated with secondary antibodies (Rhodamine Red, or FITC-conjugated donkey anti-goat or anti-rabbit IgG, Jackson ImmunoResearch) for 30 min and then counterstained with DNA dye Draq5. The cells exposed to secondary antibodies only were used as negative controls. Stained cells were viewed and imaged by Leica confocal microscope.

For colocalization analysis, the Pearson's correlation coefficient (PCC) between each pair of confocal images was calculated using the colocalization tool in ImageJ-win32 (US National Institutes of Health, Bethesda, MD). The PCC is a commonly used method to quantify the degree of colocalizaiton of two markers using immunofluorescence microscopy (Dunn et al., 2011). The negative control was provided by quantifying PCC for the same images, but after rotation of one by 90°, a condition in which only random colocalization is observed (Dunn et al., 2011). All colocalization calculations were performed on more than 20 cells from at least two independent experiments.

Endocytosis assay

Cellular endocytosis experiments were performed at 37°C in a humidified atmosphere of 5% CO_2 in air. Cells grown in 35-mm glass-bottom dishes were cultured to 90–100% confluence in growth medium, which was replaced by serum-free medium for 1 h. The cells were then incubated with FITC-BSA, AF594-BSA, or AF594-dextran for 30–60 min at 37°C. For inhibition experiments, the incubation medium also included anti-hKIM-1 antibody (AF1750: goat IgG, 10 μg/ml), anti-rKIM-1 antibody (AF3689: goat IgG, 10 μg/ml), anti-mKIM-1 antibody (AF 1817: goat IgG, 10 μg/ml), or chlorpromazine (50 μM) for 60 min before the addition of conjugated BSA. After washing in PBS (pH 7.4), cells were fixed in 4% paraformaldehyde and counterstained with Draq5. Alternatively, the fixed cells were permeabilized, blocked for nonspecific binding, exposed to primary KIM-1 antibody,

secondary antibody, and counterstained with Draq5. Cells were examined by confocal microscopy. Quantification of AF594-BSA uptake by KIM-1-positive and negative cells was performed using the ImageJ software (NIH). Fluorescence intensity is given in arbitrary units as an average value per cell in 15–20 randomly selected fields.

Extraction of membrane lipid microdomains and sucrose density gradient flotation centrifugation

Non-detergent sodium carbonate solution was used to extract lipid microdomains (Zhang et al., 2005). HK-2 cells were grown to near confluence in 100-mm^2 dishes. After two washes with ice-cold phosphate-buffered saline, two confluent dishes were scraped into 1 ml of 500 mM sodium carbonate, pH 11.0, in the presence of 1 mM PMSF and protease inhibitors cocktail. Homogenization was carried out with 10 strokes using a tight-fitting Dounce homogenizer, followed by three 20-sec bursts at 30% of maximal power to disrupt cellular membranes. The homogenates were adjusted to 45% sucrose by addition of 1 ml of 90% sucrose prepared in MBS [2-(*N*-morpholino) ethanesulfonic acid-buffered saline, 25 mM 2-(*N*-morpholino) ethanesulfonic acid, pH 6.5, and 0.15 M NaCl] and placed at the bottom of an ultracentrifuge tube. A discontinuous sucrose gradient (6 ml of 35% sucrose and 4 ml of 5% sucrose, both prepared in MBS) was formed above and centrifuged at 39,000 rpm for 20 h in an SW40 TI rotor (Beckman Instruments). A light-scattering band was observed at the 3–35% sucrose interface. Twelve 1-ml fractions were collected from the top of the tubes, and equal portion of each fraction was separated by SDS-PAGE for Western blot analysis as described above. The primary antibodies were goat anti-hKIM-1, rabbit anti-clathrin, rabbit anti-caveolin-1, and mouse anti-β-actin IgG (Sigma–Aldrich).

Subcellular localization

HK-2 cells were plated on 35 mm glass-bottom culture dishes. Following transfection with Rab5a-GFP (green), Rab7a-RFP (red), or LAMP1-GFP for 16 h, cells were fixed and then stained for hKIM-1 as described above.

Statistical analysis

Data are expressed as mean ± SEM. All experiments were performed at least three times, either with duplicates or triplicates. Statistical analysis was performed using the Student's *t*-test. A probability value of $P < 0.05$ was considered to indicate statistical significance.

Results

Albumin increased KIM-1 expression and disrupted normal cell–cell contact in primary tubular epithelial monolayer

Previous studies have demonstrated KIM-1 induction in damaged proximal tubule epithelium in proteinuric kidney diseases. To examine whether protein overload upregulates KIM-1 expression, primary cultured renal TECs were treated with albumin, the predominant type of filtered protein for tubular reabsorption. As depicted in Figure 1A, Western blot analysis revealed that KIM-1 protein was significantly increased in primary mouse TECs when exposed to albumin (10 mg/ml) for 72 h. To further determine the subcellular localization of endogenous KIM-1, we performed dual labeling for mKIM-1 and ZO-1 in

primary mouse TECs. Under normal condition, primary renal epithelial monolayer showed the presence of ZO-1 containing tight junction appearing at cell–cell contacts (Fig. 1B top). KIM-1 exhibited punctuate plasma membrane distribution and was colocalized with ZO-1 at sites of cell–cell contacts (Pearson's correlation coefficient = 0.572 ± 0.031). We verified the specificity of this calculated coefficient by rotating one channel 90° and the negative PCC was 0.003 ± 0.004 (Fig. 1C). Interestingly, an accumulation of KIM-1 in large perinuclear vesicles was observed in association with a disruption of normal cell–cell contacts as evidenced by ZO-1 redistributing from the tight junction to the cytosol when primary TECs were exposed to albumin for 72 h (Fig. 1B bottom). Moreover, KIM-1 positive cells underwent significant morphological changes being extruded from the monolayer.

KIM-1 expression increased albumin endocytosis in renal tubular cells

KIM-1 expression has been shown to increase endocytosis of lipoproteins and phagocytosis of apoptotic cells in renal TECs (Ichimura et al., 2008). To determine if KIM-1 also plays a role in tubular reabsorption of albumin, primary mouse TECs were incubated with fluorescently labeled bovine serum albumin (FITC-BSA, green), and then stained for mKIM-1. As shown in Figure 2A, FITC-BSA accumulation along the cell surface and in vesicular punctuate structures was substantially enhanced in primary TECs expressing KIM-1, whereas mild internalization of FITC-BSA was observed in mKIM-1-negative cells.

We also determined the ability of ectopic KIM-1 expression to concentrate BSA in rat NRK-52E renal tubule epithelial cell line. Similar to porcine LLC-PK1 renal tubular epithelial cell lines (Ichimura et al., 2008), NRK-52E cells do not express endogenous KIM-1. We transiently expressed full-length human KIM-1 in NRK-52E cells to examine if exogenous expression of KIM-1 can enhance albumin uptake. After transfection with hKIM-1 subcloned into pcDNA-DEST, the cells were incubated with FITC-BSA at 37°C for 30–60 min and then stained for hKIM-1. FITC-BSA intensity was significantly greater in NRK-52E cells expressing hKIM-1 compared to untransfected cells (Fig. 2B). The majority of FITC-BSA puncta were colocalized with hKIM-1 in cytoplasmic vesicles after 60-min incubation (as evidenced by PCC = 0.627 ± 0.066, Fig. 2C).

To directly visualize KIM-1 expression and BSA uptake, NRK-52E cells were also transfected with a fusion protein consisting of hKIM-1 and GFP (hKIM-GFP, green), and then incubated with Alexa Fluor 594-labeled BSA (AF594-BSA, red). When the cells were transfected with control GFP plasmid, AF594-BSA intensities did not differ significantly between green (3.20 ±0.15) and non-green (2.96 ±0.06) cells (Fig. 3A and D). As expected, a significant increase in AF594-BSA puncta was observed in NRK-52E cells expressing hKIM-GFP (Fig. 3B: no hKIM Ab). AF594-BSA intensity averaged 5.57 ±0.33 in hKIM-GFP positive versus 2.45 ± 0.05 in hKIM-GFP negative cells (Fig. 3D). To further examine if this effect is due to KIM-1 expression, we pretreated the cells with an antibody specifically targeting human KIM-1 (Fig. 3D: +hKIM Ab). Pre-incubation of transfected cells with hKIM-1 antibody significantly attenuated BSA-AF594 internalization in hKIM-GFP cells (3.39 ± 0.15), whereas BSA uptake by hKIM-1-negative cells was not affected (2.88 ± 0.07). Preincubation with the antibodies against rKIM-1 (less than 1% cross-

reactivity with hKIM-1) or against mKIM-1 (less than 5% cross-reactivity with hKIM-1) resulted in a slight decrease in albumin accumulation in hKIM-GFP cells.

To test whether KIM-1 expression affects fluid-phase endocytosis of dextran, NRK-52E cells were incubated with fluorescently labeled dextran (AF594-dextran). Following incubation with AF594-dextran for 30–60 mins, there was no difference in dextran intensities in KIM-GFP positive versus negative cells (Fig. 3C).

KIM-1 induced albumin endocytosis via a clathrin-dependent endocytic pathway

Next, we examined if KIM-1 resides in cholesterol and sphingomyelin-rich membrane rafts and if clathrin and/or caveolin-1 are co-purified with endogenous KIM-1 in renal epithelial cells. Previous studies have shown that HK-2, a human proximal tubule cell line, expresses endogenous KIM-1. Figure 4 shows that KIM-1 is predominantly found in low-density, buoyant fraction (fraction 5) of HK-2 cells fractionated by sucrose gradients in the presence of carbonate, in fractions (fractions 4–6) commonly referred to as low-density membrane rafts. Immunoblotting revealed that both caveolin-1 and clathrin were also enriched in fractions 5–6 corresponding to membrane rafts. Together, our results indicated that KIM-1 was mainly co-distributed with caveolin-1 and clathrin in membrane rafts of HK-2 cells.

The spatial relationship between KIM-1 and clathrin or caveolin-1 was further confirmed using multiple immunofluorescence labeling. Figure 5A shows that caveolin-1 was localized mainly in the peripheral area and its level varied cell by cell, whereas KIM-1 was mainly accumulated in large juxtanuclear vesicles in HK-2 cells. Moreover, less caveolin-1 expression was observed in cells with strong KIM-1 staining. In contrast, KIM-1 was extensively co-localized with clathrin in the perinuclear area with little co-localization adjacent to the plasma membrane of HK-2 cells (Fig. 5B). To confirm the role of clathrin in KIM-1 endocytic trafficking, HK-2 cells were treated with chlorpromazine. When the cells were treated with 50 mM chlorpromazine, clathrin showed a diffuse and rather homogenous fluorescence with the disappearance of juxtanuclear accumulation. Accordingly, aggregation of KIM-1 in the perinuclear area was blocked (Fig. 5B′). KIM-1 staining was observed in smaller vesicles scattered throughout the cytoplasm and clustered beneath the plasma membrane (Fig. 5B′). Since adaptor protein (AP)-2 can bind to the internalization signals of a number of membrane receptors (or their cytoplasmic tail), drawing them into coated pits and into the endocytosis process (Brown and Petersen, 1998), we assumed that inhibition of the clathrin AP-2 by chlorpromazine could cause KIM-1 accumulation at the cell surface. Figure 5C exhibits small KIM-1 and clathrin puncta with little colocalization within the plasma membrane in non-permeabilized HK-2 cells. In the presence of chlorpromazine, we often observed increased number and size of KIM-1 puncta on the cell surface, which were dissociated with clathrin-positive vesicles (Fig. 5C′). These results support that KIM-1 is constitutively endocytosed by a clathrin-dependent pathway.

Clathrin-mediated endocytosis plays a major role in internalization of various receptors and ligands. A recent report indicates that KIM-1 is constitutively endocytosed through clathrin-mediated vesicles in different epithelial cell lines (Balasubramanian et al., 2012). To further determine if clathrin is required for KIM-1-mediated albumin internalization, the effect of chlorpromazine on FITC-BSA uptake was evaluated in hKIM-NRK cells. As shown in

Figure 6, albumin internalization was almost abolished by chlorpromazine in both untransfected and hKIM-1-transfected NRK-52E cells, indicating that clathrin-dependent process is involved in KIM-1-mediated albumin internalization by renal tubular epithelial cells. An increase in albumin internalization was accompanied by the formation of large lysosome-like vacuoles in hKIM-NRK cells (Fig. 6 top, DIC: differential interference contrast) upon albumin stimulation. These large vacuoles were usually labeled with KIM-1 and mostly clustered around the nucleus. Pre-incubation of transfected cells with chlorpromazine resulted in the formation of a few giant vacuoles with concomitant disappearance of smaller ones in hKIM-NRK cells upon albumin stimulation (Fig. 6 bottom, DIC), which was not observed in hKIM-negative NRK-52E cells. These giant vacuoles appeared on the cell surface with localization of KIM-1 to the vacuolar membrane.

KIM-1 and its protein cargo localize to endocytic/lysosomal compartments

To confirm whether the vesicular structures associated with KIM-1 were endosomes, we transfected HK-2 cells with Rab5a-GFP, Rab7a-RFP, or LAMP1-GFP for 16 h and then stained for hKIM-1. As shown in Figure 7, Rab5a-positive early endosomes were partly present throughout the cytoplasm and partly concentrated in the perinuclear region, whereas Rab7a-positive late endosomes was mainly accumulated in the perinuclear region. An association of KIM-1 with early and late endosomes was revealed by confocal microscopy, which detected KIM-1 in juxtanuclear vesicles positive for Rab5a (Fig. 7A) or Rab7a (Fig. 7B). An association of KIM-1 with lysosomes was also indicated by colocalization of KIM-1 with the lysosomal marker LAMP1 (Fig. 7C). Similar results were seen in 769-P, a human kidney carcinoma cell line. When 769-P cells were transiently transfected with LAMP1-GFP, some LAMP1-positive cells developed large vacuoles with colocalization of KIM-1 and LAMP1 on the vacuolar membrane (data not shown). We also observed that albumin internalization led to an increase in lysosomal activity, which was reflected by increased lysotracker staining, a dye selectively accumulating in acidic compartments (Fig. 7D). Together, these data support that KIM-1 and its cargo protein traffic through early and late endosomal/multivesicular compartments and are ultimately delivered to lysosomes.

KIM-1 expression is suppressed by TGF-β1 in tubular epithelial cells

TGF-β1 has been shown to downregulate the expression of albumin binding receptor megalin and inhibit albumin uptake in renal tubule epithelial cells (Gekle et al., 2003; Russo et al., 2007). Next, we performed Western blot and immunostaining analyses to evaluate the effect of TGF-β1 on KIM-1 expression in renal tubular cells. As expected, TGF-β1 administration(1 or 2 ng/ml, 24 h) resulted in an increase in Smad-3 phosphorylation in HK-2 cells (Fig. 8A). Meanwhile, KIM-1 and E-cadherin protein levels were significantly reduced following TGF-β1 treatment for 24 or 48 h (Fig. 8B). Confocal microscopy confirmed a decrease in KIM-1 staining in TGF-β1-treated HK-2 cells (Fig. 8). Similar changes to TGF-β1 treatment were also detected in primary cultures of mouse and rat renal TECs (data not shown).

Discussion

We have previously reported that KIM-1 is gradually induced in activated proximal tubules, in association with the levels of urinary protein/albumin, in a rat model of type 2 diabetes (Zhao et al., 2011). In this report, we show that KIM-1 expression enhances albumin uptake by renal TECs. KIM-1-induced albumin endocytosis appears to be mediated by a clathrin-dependent pathway. This is supported by a colocalization of KIM-1 and clathrin in the intracellular vesicles and blockade of KIM-1-mediated albumin internalization by chlorpromazine, an inhibitor of clathrin-dependent endocytosis.

KIM-1 is upregulated and acts as a receptor for lipoproteins and apoptotic cells in activated renal proximal tubules (Ichimura et al., 2008). Our results extend these observations by showing that KIM-1 expression enhances albumin internalization in renal tubular cells. Using fluorescence microscopy, we directly compared albumin uptake by KIM-1 positive versus negative cells, since the cell monolayer consists of both KIM-1-positive and negative cells that are exposed to the same quality and quantity of fluorescently-labeled protein. We consistently observed that fluorescently conjugated BSA accumulated in primary mouse TECs expressing endogenous KIM-1. Overexpressing human KIM-1 in NRK-52E cell line also enhanced albumin uptake, which was prevented by specific KIM-1 antibody. An inability to stimulate the uptake of fluid-phase marker dextran supports that KIM-1 expression specifically enhanced receptor-mediated albumin endocytosis in renal TECs. However, the data do not allow the conclusion that KIM-1 is itself an albumin receptor. It also remains possible that KIM-1 binds to moieties such as fatty acids carried by albumin and/or other proteins, rather than the protein itself. This issue is currently under study in our laboratory.

Clathrin-dependent endocytosis is a well-understood receptor-mediated endocytic pathway, which occurs constitutively in all mammalian cells and carries out continuous uptake of proteins and nutrients. A recent report has indicated that KIM-1 itself is constitutively endocytosed through clathrin-mediated vesicles in different epithelial cell lines (Balasubramanian et al., 2012). Therefore, we assumed that KIM-1 may increase albumin uptake via a clathrin-dependent mechanism. This concept was confirmed by the observations that KIM-1 and clathrin was colocalized in the juxtanuclear vesicles in renal TECs and that KIM-1-induced albumin accumulation was inhibited by chlorpromazine treatment. Following albumin stimulation, KIM-1 positive NRK-52E cells exhibited increased formation of lysosome-like vacuoles. Inhibition of clathrin-dependent endocytic pathway with chlorpromazine led to the formation of a few giant vacuoles with concomitant disappearance of smaller ones in hKIM-NRK cells. These giant vacuoles appeared on the cell surface with localization of KIM-1 to the vacuolar membrane. It is possible that ligand activation of KIM-1 increases the propensity for the membrane to undergo fusion, leading to the formation of large lysosome-like vacuoles by accelerating the fusion of smaller vesicles to the growing endosomes through a clathrin-dependent pathway. Blockade of clathrin-mediated endocytic pathway by chlorpromazine inhibits the clathrin-mediated membrane from budding and pinching off from plasma membrane but may not affect KIM-1-mediated vacuolar membrane fusion, triggering the generation of giant vacuoles at the cell surface. To gain further insight into compartmental distribution of KIM-1 and the fate of internalized

protein, we performed colocalization studies with KIM-1 and specific markers of the endosomal and lysosomal pathways. We found that KIM-1 codistributed with early endosome marker Rab5, late endosomal marker Rab7, and lysosomal marker LAMP1. In canonical receptor-mediated endocytosis, early endosomes mature into late endosomes, multivesicular bodies, and lysosomes (Luzio et al., 2009a; 2009b). Therefore, the proteins internalized by KIM-1 cells are most probably sorted into a lysosomal compartment for final degradation.

It is of importance that KIM-1 enhances albumin uptake and delivery to the lysosomes as many reports have validated changes in the levels of different inflammatory proteins and transcription factors in response to protein load and lysosomal protein accumulation in the proximal tubule (Abbate et al., 2006). Various mechanisms have been proposed to explain the link between proteinuria, tubulointerstitial injury, and progressive chronic renal failure (Nath, 1992). Some authors postulate that albuminuria may exert a toxic effect on renal TEC, thus damaging the cells and initiating the process of interstitial fibrosis and scarring (Thomas and Schreiner, 1993; Burton and Harris, 1996). The nephrotoxicity of albuminuric states may be not only due to the protein molecule itself but that the toxicity resides in lipid carried on albumin. For example, Thomas et al. (2002) have shown that renal tubulointerstitial lesion is markedly more severe in animals injected with fatty acid-bearing BSA than in those injected with fatty acid-free BSA, despite comparable levels of proteinuria in both groups. Filtered albumin presents fatty acids to proximal tubule epithelial cells in large quantities by an unusual and unregulated apical route in most proteinuric kidney diseases including diabetic nephropathy. Thus, KIM-1 induction on the apical membrane may contribute to tubulointerstitial inflammation and fibrosis by enhancing the deleterious effects of these stimuli on proximal tubule cells. This concept is supported by the report that KIM-1 positive tubules were located mainly in the tubulointerstitial regions affected by inflammation or fibrosis in patients with different kidney diseases (Simic Ogrizovic et al., 2013). We also found that KIM-1-positive tubules were often surrounded by increased interstitial myofibroblasts revealed by strong interstitial staining for desmin and alpha-smooth muscle actin in the kidney of diabetic rats (data not shown). Future studies are warranted to further evaluate the role of KIM-1-induced albumin uptake in tubular dysfunction and renal fibrosis under proteinuric condition.

In proteinuria, KIM-1 expression is dynamically upregulated in renal proximal tubules. A direct stimulatory effect of albumin on KIM-1 expression was confirmed in primary cultured renal TECs derived from mouse and rat (data not shown) kidney tissues. In contrast, TGF-β1 produced an inhibitory effect on KIM-1 expression in renal TECs, which is similar to the previous finding that TGF-β1 downregulates the expression of albumin binding receptor megalin and inhibit albumin uptake in renal tubule epithelial cells (Gekle et al., 2003; Russo et al., 2007).

In conclusion, a new functional role of tubular KIM-1 was identified as an enhancer of luminal albumin trafficking under proteinuric conditions. KIM-1-induced albumin uptake was mediated by clathrin-dependent endocytic pathway, since albumin accumulation was effectively inhibited by chlorpromazine. Furthermore, because albumin by itself stimulates KIM-1 expression in cultured renal TECs, it is speculated that uptake of albumin would be

increased, with great potential to accelerate renal injury induced by protein overload. Therefore, KIM-1 appears to be closely associated with tubular injury and renal dysfunction. Tubular KIM-1 may be a logical therapeutic target to prevent progressive renal functional loss in proteinuric nephropathies.

Acknowledgments

This work was supported by the NIH SDK096441, NIH/ NCRR/RCMI 8G12MD007602 and 8U54MD007588.

Contract grant sponsor: NIH SDK096441, NIH/NCRR/RCMI

Contract grant numbers: 8G12MD007602, 8U54MD007588.

Literature Cited

Abbate M, Zoja C, Remuzzi G. How does proteinuria cause progressive renal damage? J Am Soc Nephrol: JASN. 2006; 17:2974–2984. [PubMed: 17035611]

Amsellem S, Gburek J, Hamard G, Nielsen R, Willnow TE, Devuyst O, Nexo E, Verroust PJ, Christensen EI, Kozyraki R. Cubilin is essential for albumin reabsorption in the renal proximal tubule. J Am Soc Nephrol: JASN. 2010; 21:1859–1867. [PubMed: 20798259]

Baines RJ, Chana RS, Hall M, Febbraio M, Kennedy D, Brunskill NJ. CD36 mediates proximal tubular binding and uptake of albumin and is upregulated in proteinuric nephropathies. Am J Physiol Renal Physiol. 2012; 303:F1006–F1014. [PubMed: 22791331]

Balasubramanian S, Kota SK, Kuchroo VK, Humphreys BD, Strom TB. TIM family proteins promote the lysosomal degradation of the nuclear receptor NUR77. Sci Signal. 2012; 5:ra90. [PubMed: 23233528]

Birn H, Fyfe JC, Jacobsen C, Mounier F, Verroust PJ, Orskov H, Willnow TE, Moestrup SK, Christensen EI. Cubilin is an albumin binding protein important for renal tubular albumin reabsorption. J Clin Invest. 2000a; 105:1353–1361. [PubMed: 10811843]

Birn H, Vorum H, Verroust PJ, Moestrup SK, Christensen EI. Receptor-associated protein is important for normal processing ofmegalinin kidney proximal tubules. J AmSoc Nephrol: JASN. 2000b; 11:191–202.

Bonventre JV. Kidney injury molecule-1 (KIM-1): Aurinary biomarker and much more. Nephrol Dial Transplant. 2009; 24:3265–3268. [PubMed: 19318357]

Brown CM, Petersen NO. An image correlation analysis of the distribution of clathrin associated adaptor protein (AP-2) at the plasma membrane. J Cell Sci. 1998; 111:271–281. [PubMed: 9405317]

Burton C, Harris KP. The role ofproteinuriain the progressionof chronic renal failure. Am J Kidney Dis. 1996; 27:765–775. [PubMed: 8651239]

Chaturvedi S, Farmer T, Kapke GF. Assay validation for KIM-1: Human urinary renal dysfunction biomarker. Int J Biol Sci. 2009; 5:128–134. [PubMed: 19173034]

Christensen EI, Birn H. Megalin and cubilin: Multifunctional endocytic receptors. Nat Rev Mol Cell Biol. 2002; 3:256–266. [PubMed: 11994745]

Christensen EI, Moskaug JO, Vorum H, Jacobsen C, Gundersen TE, Nykjaer A, Blomhoff R, Willnow TE, Moestrup SK. Evidence for an essential roleof megalin in transepithelial transport of retinol. J Am Soc Nephrol: JASN. 1999; 10:685–695. [PubMed: 10203351]

Christensen EI, Willnow TE. Essential role of megalin in renal proximal tubule for vitamin homeostasis. J Am Soc Nephrol: JASN. 1999; 10:2224–2236. [PubMed: 10505701]

Conner SD, Schmid SL. Regulated portals of entry into the cell. Nature. 2003; 422:37–44. [PubMed: 12621426]

Dunn KW, Kamocka MM, McDonald JH. A practical guide to evaluating colocalization in biological microscopy. Am J Physiol Cell Physiol. 2011; 300:C723–C742. [PubMed: 21209361]

Erkan E, De Leon M, Devarajan P. Albumin overload induces apoptosis in LLC-PK(1) cells. Am J Physiol Renal Physiol. 2001; 280:F1107–F1114. [PubMed: 11352849]

Gekle M. Renal proximal tubular albumin reabsorption: Daily prevention of albuminuria. News Physiol Sci. 1998; 13:5–11. [PubMed: 11390751]

Gekle M. Renal tubule albumin transport. Annu Rev Physiol. 2005; 67:573–594. [PubMed: 15709971]

Gekle M, Knaus P, Nielsen R, Mildenberger S, Freudinger R, Wohlfarth V, Sauvant C, Christensen EI. Transforming growth factor-beta1 reduces megalin- and cubilin-mediated endocytosis of albumin in proximal-tubule-derived opossum kidney cells. J Physiol. 2003; 552:471–481. [PubMed: 14561830]

Gekle M, Mildenberger S, Freudinger R, Schwerdt G, Silbernagl S. Albumin endocytosis in OK cells: Dependence on actin and microtubules and regulation by protein kinases. Am J Physiol. 1997; 272:F668–F677. [PubMed: 9176379]

Ichimura T, Asseldonk EJ, Humphreys BD, Gunaratnam L, Duffield JS, Bonventre JV. Kidney injury molecule-1 is a phosphatidylserine receptor that confers a phagocytic phenotype on epithelial cells. J Clin Invest. 2008; 118:1657–1668. [PubMed: 18414680]

Kramer AB, van der Meulen EF, Hamming I, van Goor H, Navis G. Effect of combining ACE inhibition with aldosterone blockade on proteinuria and renal damage in experimental nephrosis. Kidney Int. 2007; 71:417–424. [PubMed: 17213874]

Kramer AB, van Timmeren MM, Schuurs TA, Vaidya VS, Bonventre JV, van Goor H, Navis G. Reduction of proteinuria in adriamycin-induced nephropathy is associated with reduction of renal kidney injury molecule (Kim-1) over time. Am J Physiol Renal Physiol. 2009; 296:F1136–F1145. [PubMed: 19225054]

Kuehn EW, Park KM, Somlo S, Bonventre JV. Kidney injury molecule-1 expression in murine polycystic kidney disease. Am J Physiol Renal Physiol. 2002; 283:F1326–F1336. [PubMed: 12388382]

Li L, Emmett N, Mann D, Zhao X. Fenofibrate attenuates tubulointerstitial fibrosis and inflammation through suppression of nuclear factor-kappaB and transforming growth factor-beta1/Smad3 in diabetic nephropathy. Exp Biol Med (Maywood). 2010; 235:383–391. [PubMed: 20404057]

Luzio JP, Parkinson MD, Gray SR, Bright NA. The delivery of endocytosed cargo to lysosomes. Biochem Soc Trans. 2009a; 37:1019–1021. [PubMed: 19754443]

Luzio JP, Piper SC, Bowers K, Parkinson MD, Lehner PJ, Bright NA. ESCRT proteins and the regulation of endocytic delivery to lysosomes. Biochem Soc Trans. 2009b; 37:178–180. [PubMed: 19143626]

Motoyoshi Y, Matsusaka T, Saito A, Pastan I, Willnow TE, Mizutani S, Ichikawa I. Megalin contributes to the early injury of proximal tubule cells during nonselective proteinuria. Kidney Int. 2008; 74:1262–1269. [PubMed: 18769366]

Mukherjee S, Ghosh RN, Maxfield FR. Endocytosis. Physiol Rev. 1997; 77:759–803. [PubMed: 9234965]

Nath KA. Tubulointerstitial changes as a major determinant inthe progressionof renal damage. Am J Kidney Dis. 1992; 20:1–17. [PubMed: 1621674]

Nielsen R, Mollet G, Esquivel EL, Weyer K, Nielsen PK, Antignac C, Christensen EI. Increased lysosomal proteolysis counteracts protein accumulation in the proximal tubule during focal segmental glomerulosclerosis. Kidney Int. 2013; 84:902–910. [PubMed: 23760285]

Remuzzi G, Bertani T. Pathophysiology of progressive nephropathies. N Engl J Med. 1998; 339:1448–1456. [PubMed: 9811921]

Russo LM, del Re E, Brown D, Lin HY. Evidence for a role of transforming growth factor (TGF)-beta1 in the induction of postglomerular albuminuria in diabetic nephropathy: Amelioration by soluble TGF-beta type II receptor. Diabetes. 2007; 56:380–388. [PubMed: 17259382]

Sandbichler AM, Aschberger T, Pelster B. A method to evaluate the efficiency of transfection reagents in an adherent zebrafish cell line. Biores Open Access. 2013; 2:20–27. [PubMed: 23515475]

Schmid SL. Clathrin-coated vesicle formation and protein sorting: An integrated process. Annu Rev Biochem. 1997; 66:511–548. [PubMed: 9242916]

Simic OS, Bojic S, Basta-Jovanovic G, Radojevic S, Pavlovic J, Kotur SJ, Dopsaj V, Naumovic R. Tissue kidney injury molecule-1 expression in the prediction of renal function for several years after kidney biopsy. Dis Markers. 2013; 35:567–572. [PubMed: 24282337]

Thomas ME, Harris KP, Walls J, Furness PN, Brunskill NJ. Fatty acids exacerbate tubulointerstitial injury in protein-overload proteinuria. Am J Physiol Renal Physiol. 2002; 283:F640–F647. [PubMed: 12217854]

Thomas ME, Schreiner GF. Contribution of proteinuria to progressive renal injury: Consequences of tubular uptake of fatty acid bearing albumin. Am J Nephrol. 1993; 13:385–398. [PubMed: 8116691]

van Timmeren MM, Bakker SJ, Vaidya VS, Bailly V, Schuurs TA, Damman J, Stegeman CA, Bonventre JV, van Goor H. Tubular kidney injury molecule-1 in protein-overload nephropathy. Am J Physiol Renal Physiol. 2006; 291:F456–F464. [PubMed: 16467126]

Verroust PJ, Kozyraki R. The roles of cubilin and megalin, two multiligand receptors, in proximal tubule function: Possible implication in the progression of renal disease. Curr Opin Nephrol Hypertens. 2001; 10:33–38. [PubMed: 11195049]

Wang Y, Chen J, Chen L, Tay YC, Rangan GK, Harris DC. Induction of monocyte chemoattractant protein-1 in proximal tubule cells by urinary protein. J Am Soc Nephrol. 1997; 8:1537–1545. [PubMed: 9335381]

Zeng Y, Yang X, Wang J, Fan J, Kong Q, Yu X. Aristolochic acid I induced autophagy extenuates cell apoptosis via ERK 1/2 pathway in renal tubular epithelial cells. PLoS One. 2012; 7:e30312. [PubMed: 22276178]

Zhai XY, Nielsen R, Birn H, Drumm K, Mildenberger S, Freudinger R, Moestrup SK, Verroust PJ, Christensen EI, Gekle M. Cubilin- and megalin-mediated uptake of albumin in cultured proximal tubule cells of opossum kidney. Kidney Int. 2000; 58:1523–1533. [PubMed: 11012887]

Zhang XL, Topley N, Ito T, Phillips A. Interleukin-6 regulation of transforming growth factor (TGF)-beta receptor compartmentalization and turnover enhances TGF-beta1 signaling. J Biol Chem. 2005; 280:12239–12245. [PubMed: 15661740]

Zhao X, Zhang Y, Li L, Mann D, Imig JD, Emmett N, Gibbons G, Jin LM. Glomerular expression of kidney injury molecule-1 and podocytopenia in diabetic glomerulopathy. Am J Nephrol. 2011; 34:268–280. [PubMed: 21822010]

Zoja C, Donadelli R, Colleoni S, Figliuzzi M, Bonazzola S, Morigi M, Remuzzi G. Protein overload stimulates RANTES production by proximal tubular cells depending on NF-kappa B activation. Kidney Int. 1998; 53:1608–1615. [PubMed: 9607191]

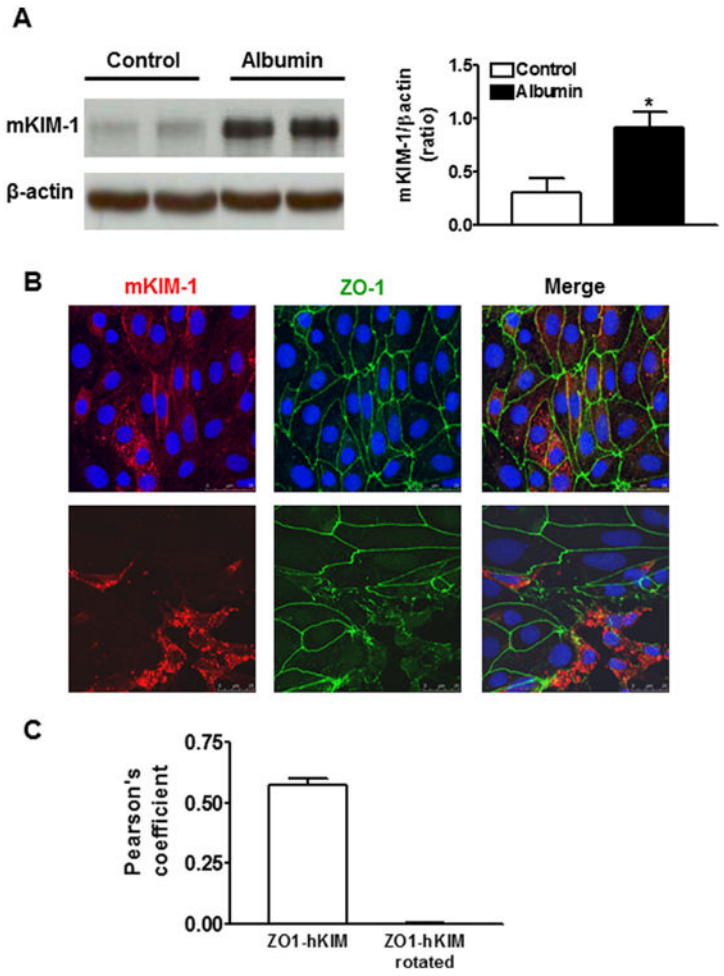

Fig. 1.

KIM-1 protein expression in primary cultures of mouse tubular epithelial cells (TECs) following albumin stimulation. A: KIM-1 protein level was significantly increased when the primary mouse renal TECs were incubated with bovine serum albumin (10 mg/ml) for 72 h. An n of 3–4 epithelial cultures were treated for each condition; $*P < 0.05$ versus untreated control group. B: Double immunostaining for mKIM-1 and Zonula Occludens (ZO-1) show that mKIM-1 red staining was present at the cell-cell border (green ZO-1) and in small intracellular vesicles in untreated primary TECs (top). Following albumin stimulation for 72 h, mKIM-1 was concentrated in large perinuclear vesicles in association with a disruption of cell–cell contacts (bottom). Images are Z-stack projections. C: Quantification of co-localization of images as in panel B top using Pearson's correlation coefficient (PCC). The negative control was provided by quantifying PCC for the same images, but after rotation of one by 90°. The results represent more than 20 cells from at least n = 2 independent experiments.

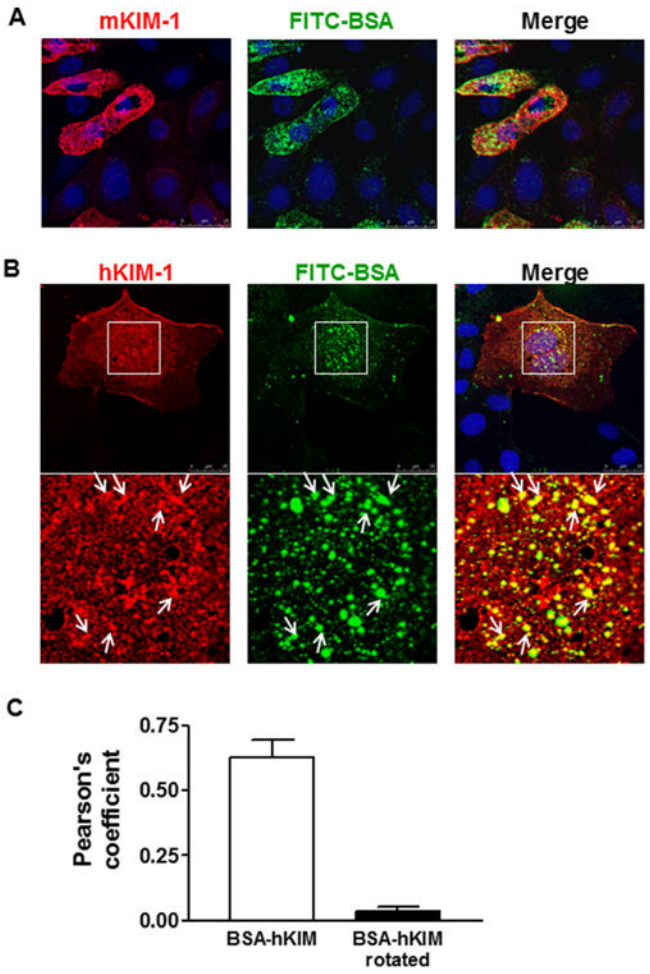

Fig. 2.

Effect of KIM-1 expression on internalization of FITC-BSA by renal tubular cells. A: Primary mouse renal TECs were incubated with FITC-labeled bovine serum albumin (FITC-BSA, 100 μg/ml, green) for 1 h and then stained for mouse KIM-1 (mKIM-1, red). Representative confocal images show an accumulation of FITC-BSA in mKIM-1 positive cells. B: NRK-52E cell line was transfected with human KIM-1 (hKIM-1) subcloned into pcDNA-DEST. Following transfection for 48 h, the cells were incubated with FITC-BSA (green) at 37°C for 1 h and then stained for hKIM-1 (red). FITC-BSA signal was markedly enhanced in hKIM-1-positive cells compared to negative ones. Additionally, BSA-FITC and hKIM-1 were strongly co-localized with one another in the intracellular vesicles (arrows). Staining was repeated at least three times with similar results. Images are Z-stack projections. C: Quantification of co-localization from images in panel B using Pearson's correlation coefficient (PCC). The negative control was provided by quantifying PCC for the same images, but after rotation of one by 90°. The results represent more than 20 cells from at least n = 2 independent experiments.

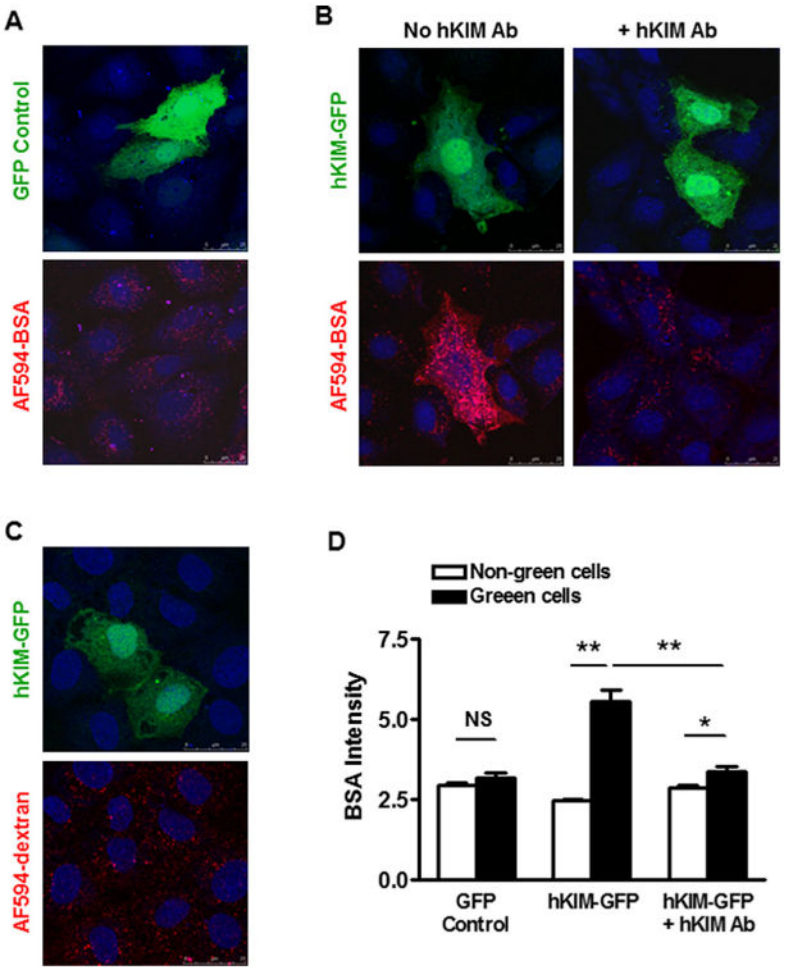

Fig. 3.

KIM-1 mediated endocytosis of albumin was inhibited by specific KIM-1 antibody. A: NRK-52E cells were transfected with control GFP (green) plasmid for 48 h and then incubated with AF594-BSA (red) for 1 h. AF594-BSA intensities did not differ significantly between GFP positive (green) cells and negative (non-green) ones. B: Following transfection of NRK-52E cells with a fusion protein consisting of hKIM-1 and GFP (hKIM-GFP), AF594-BSA was accumulated in hKIM-GFP cells compared to hKIM-GFP negative ones (B: no hKIM Ab). Pre-incubation of the transfected cells with specific hKIM-1 antibody markedly inhibited AF594-BSA accumulation in hKIM-GFP cells, but it had no effect on endocytosis of AF594-BSA by hKIM-GFP-negative cells (B: +hKIM Ab). Staining was repeated at least three times with similar results. Images are Z-stack projections. C: AF594-dextran intensities were not different in hKIM-GFP-positive versus negative NRK-52E cells. D: Quantification of AF594-BSA fluorescence was done using the ImageJ Software directly on the microscopic images of labeled cells. n = 20–50 cells per group. $*P < 0.01$, $**P < 0.001$.

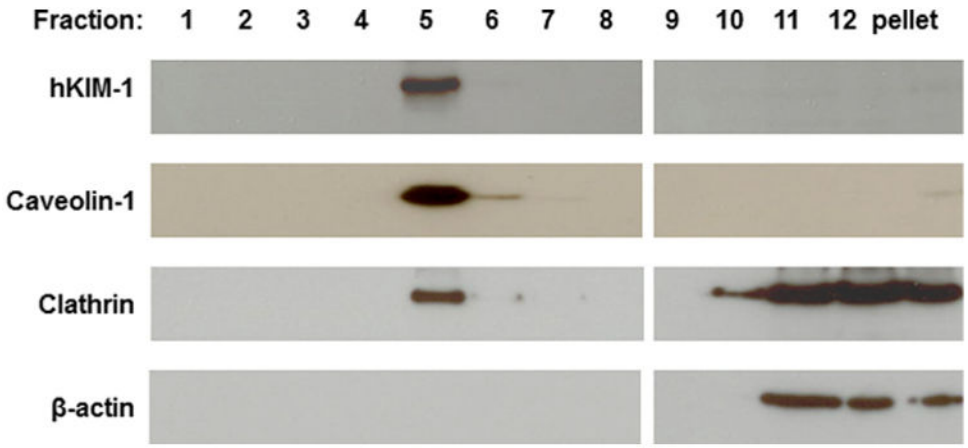

Fig. 4.

Localization of KIM-1 protein in lipid microdomains in HK-2 cells. Membrane fractions were prepared from the HK-2 cells using non-detergent sodium carbonate extraction and sucrose density gradient separation. Twenty-five microliter of each fraction (1–12) was added on SDS-PAGE gels and proteins were detected by Western blot. KIM-1 was colocalized with caveolin-1 and clathrin to the lipid raft domains.

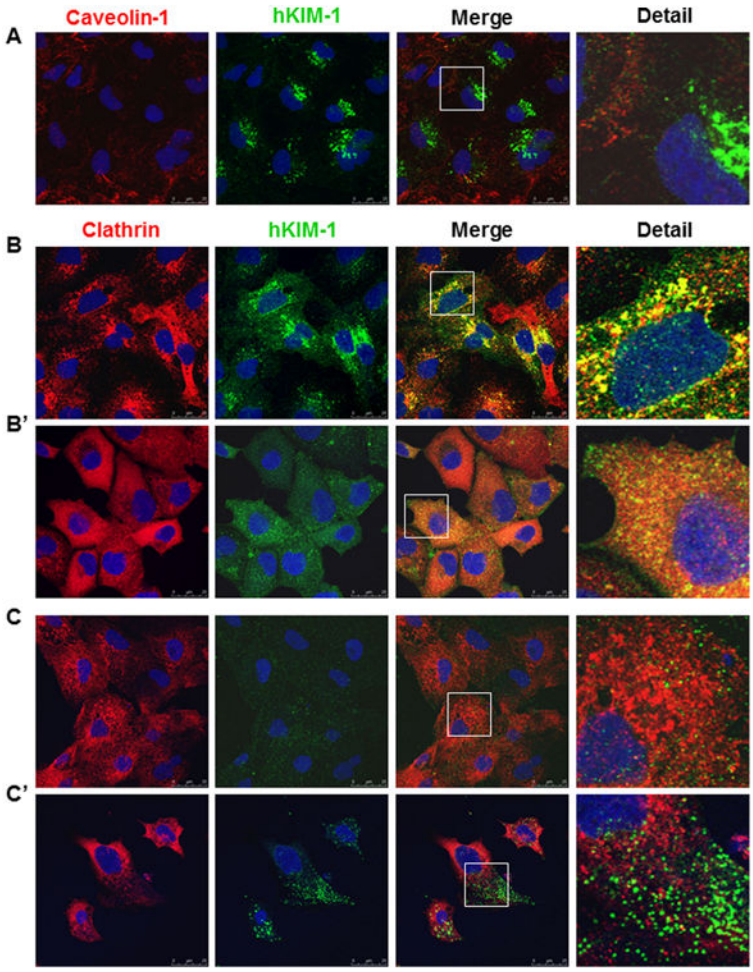

Fig. 5.

Colocalization of KIM-1 with clathrin in renal tubular epithelial cells. A: There was no significant colocalization between KIM-1 and caveolin-1 in HK-2 cells. B: A colocalization of KIM-1 and clathrin was evident in the perinuclear area of HK-2 cells. Removal of AP2 from the plasma membrane by chlorpromazine markedly increased the lateral diffusion of clathrin and KIM-1 (B′) compared to their predominant perinuclear localization in the absence of chlorpromazine (B). C–C′: In non-permeabilized HK-2 cells, chlorpromazine administration increased the number and size of KIM-1 puncta on the cell surface (C′) compared to untreated cells (C). Staining was repeated at least three times with similar results. Images are Z-stack projections.

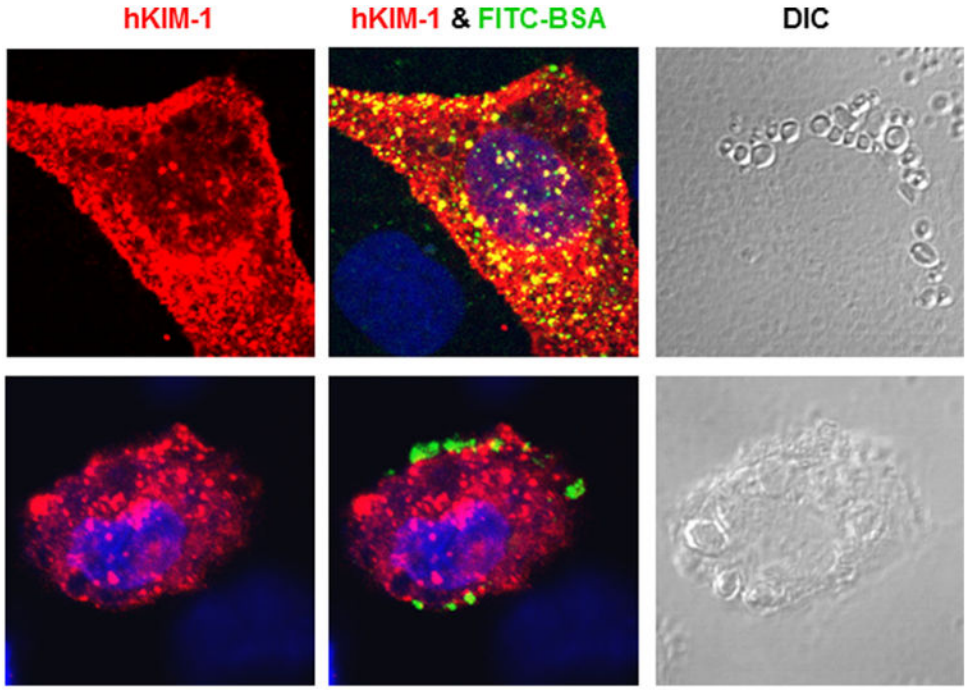

Fig. 6.

KIM-1-mediated albumin uptake was inhibited by chlorpromazine. hKIM-1-transfected NRK-52E cells were incubated with FITC-BSA (100 μg/ml) at 37°C in the absence (top) or presence (bottom) of chlorpromazine. Administration of chlorpromazine inhibited FITC-BSA accumulation in hKIM-1-positive cells, which was associated with an appearance of abnormally giant vacuoles on the cell surface. Staining was repeated at least three times with similar results. Images are Z-stack projections.

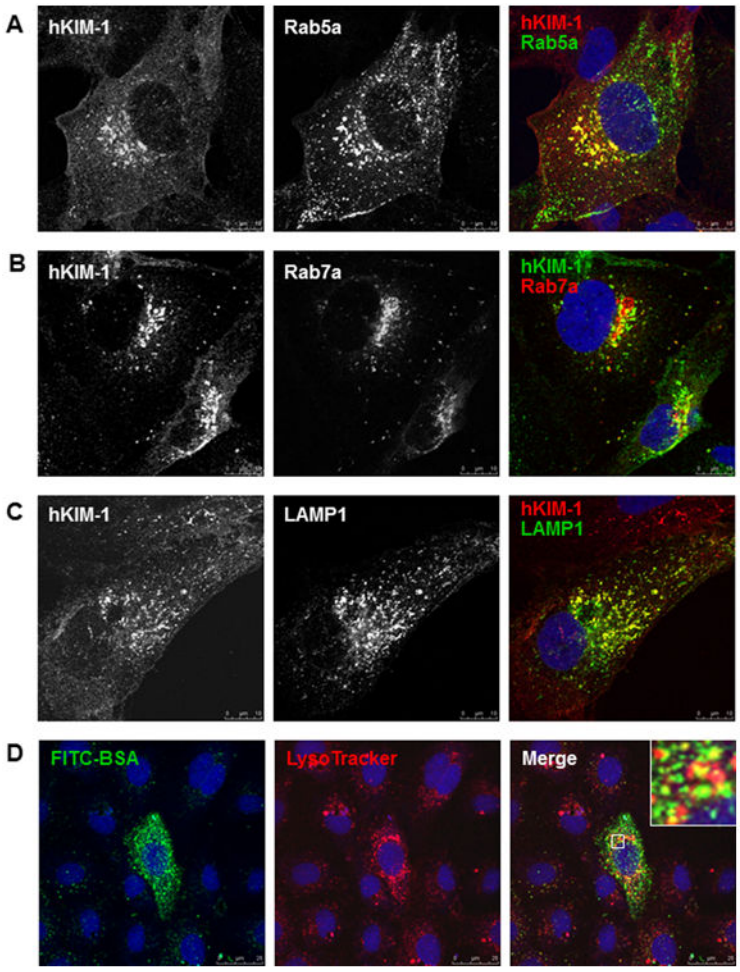

Fig. 7.

Endocytic trafficking of endogenous KIM-1 in HK-2 cells. A–C: HK-2 cells were transfected with a plasmid encoding GFP-Rab5a, RFP-Rab7a, or GFP-LAMP1 for 16 h and then immunostained with a goat anti-hKIM-1 antibody. Representative confocal images show colocalization of KIM-1 with early endosomes (A, Rab5a), late endosomes (B, Rab7a), and lysosomes (C, LAMP1). D: hKIM-1-transfected NRK-52E cells were incubated with FITC-BSA (green) and LysoTracker (red) for 30 min at 37°C. A distribution of BSA in acidic lysosomal compartments was evident in the merged image (yellow). Staining was repeated three times with similar results. Images are Z-stack projections.

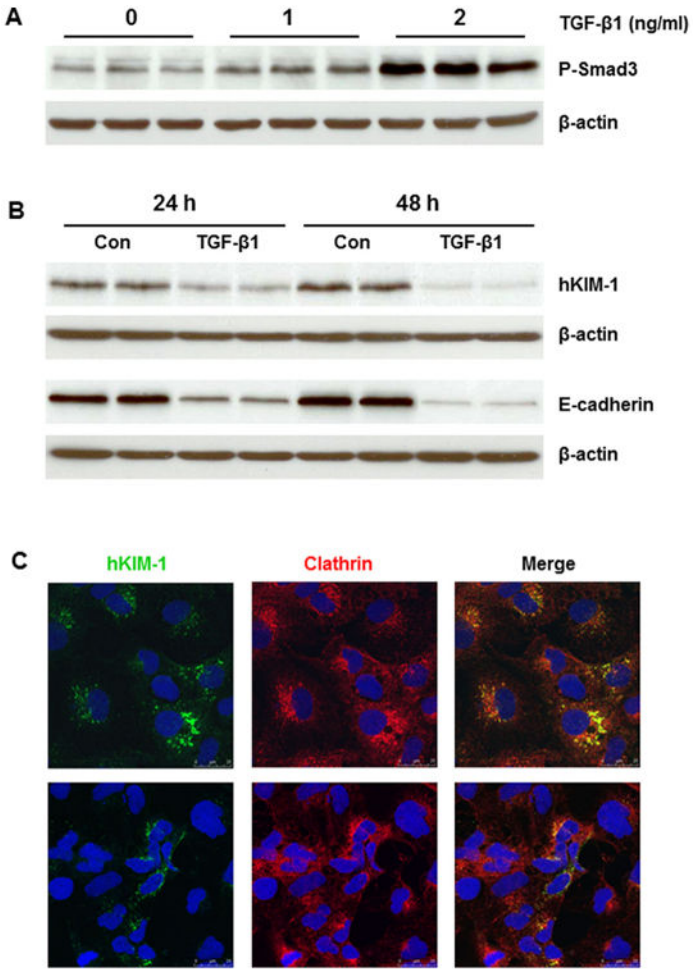

Fig. 8.

Effect of TGF-β1 on KIM-1 protein in HK-2 cells. A: TGF-β1 (1 and 2 ng/ml) led to a dose-dependent increase of Smad3 phosphorylation in HK-2 cells after 24 h. B: TGF-β1 (2 ng/ml) significantly reduced hKIM-1 and E-cadherin protein levels after 24 and 48 h. C: Representative confocal images show that hKIM-1 staining was reduced in HK-2 cells treated with TGF-β1 (2 ng/ml) for 24 h (bottom) compared to untreated cells (top).